



**HAL**  
open science

## Highly transparent piezoelectric PZT membranes for transducer applications

Franklin Pavageau, Christel Dieppedale, Pierre Perreau, Romain Liehti, Antoine Hamelin, Christophe Licitra, Fabrice Casset, Gwenael Le Rhun

► **To cite this version:**

Franklin Pavageau, Christel Dieppedale, Pierre Perreau, Romain Liehti, Antoine Hamelin, et al.. Highly transparent piezoelectric PZT membranes for transducer applications. Sensors and Actuators A: Physical , 2022, <https://doi.org/10.1016/j.sna.2022.113866>. cea-03791813

**HAL Id: cea-03791813**

**<https://cea.hal.science/cea-03791813>**

Submitted on 4 Oct 2022

**HAL** is a multi-disciplinary open access archive for the deposit and dissemination of scientific research documents, whether they are published or not. The documents may come from teaching and research institutions in France or abroad, or from public or private research centers.

L'archive ouverte pluridisciplinaire **HAL**, est destinée au dépôt et à la diffusion de documents scientifiques de niveau recherche, publiés ou non, émanant des établissements d'enseignement et de recherche français ou étrangers, des laboratoires publics ou privés.

# Highly transparent piezoelectric PZT membranes for transducer applications

Franklin Pavageau\*, Christel Dieppedale, Pierre Perreau, Romain Liechti, Antoine Hamelin, Christophe Licitra, Fabrice Casset, Gwenaël Le Rhun\*

Univ. Grenoble Alpes, CEA, Leti, F-38000 Grenoble, France

\*corresponding authors: [franklin.pavageau@cea.fr](mailto:franklin.pavageau@cea.fr) (F. Pavageau), [gwenael.le-rhun@cea.fr](mailto:gwenael.le-rhun@cea.fr) (G. Le Rhun)

## ABSTRACT

Transparent PZT-based membranes were fabricated out of 200 mm silicon wafers thanks to an innovative layer transfer process. The ITO (100 nm)/PZT (1.16  $\mu\text{m}$ )/ITO (150 nm)/SiO<sub>2</sub> (8.7  $\mu\text{m}$ ) membrane stack shows an average transmission of about 75 % in the visible spectrum. PZT film is highly (100) oriented and measured capacitors exhibit ferroelectric, dielectric and piezoelectric properties comparable to standard non-transparent PZT with metal electrodes. Piezoelectric actuation under applied voltage was verified through both static deflection and acoustic measurements. This first proof of concept opens the way to the fabrication of transparent piezoelectric transducers such as transparent PMUT devices.

Keywords: Piezoelectric, Transducer, Thin film, PZT, Transparent, Membrane

## 1. Introduction

Lead zirconate titanate, Pb(Zr,Ti)O<sub>3</sub> (PZT), has been the most studied piezoelectric thin film material for MEMS actuators the last two decades, due to its high transverse piezoelectric coefficient  $d_{31}$  [1,2]. The PZT technology is now available in several MEMS foundries and thin film PZT actuators are already integrated in commercialized devices like inkjet printheads, micro-speakers and autofocus cameras. Emerging applications such as micro-mirror for LIDAR, haptics for human-machine interfaces, micro-pumps, as well as PMUT for fingerprint, medical probe or gesture recognition are also based on thin film PZT actuators [3]. In recent years, transparent piezoelectric thin films are showing growing interest for transducers and actuator functions in application domains like photoacoustic imaging [4-6], haptics [7,8] and acoustics [9].

To obtain transparent piezoelectric stack, PZT, which is transparent due to its large bandgap (3.35 eV) [10], must be integrated on transparent elastic membrane (e.g. SiO<sub>2</sub>) with transparent electrodes. However, in the case of PZT films, the standard growth process for getting optimal piezoelectric performances requires high crystallization temperature (typically 650-700°C), non-transparent Pt bottom electrode and Si substrate. Growth of PZT with good piezoelectric properties on transparent electrode coated SiO<sub>2</sub> membrane is made difficult due to its high crystallization temperature. Indeed, the diffusion of Pb towards the substrate as well as the degradation of both electrical conductivity and transparency of the electrode must be seriously considered. In particular, it is very challenging to grow oriented PZT on non-Pt electrode, which is by far the most used. Indium tin oxide (ITO) is among the best candidates as transparent electrode material, but it is known to degrade at temperature above 300°C [11,12]. Fluorine doped tin oxide (FTO) shows better resistance to temperature than ITO and is thus often preferred for growing PZT films [13,14]. Ueda et al. annealed sputtered and sol-gel deposited PZT on FTO/glass at temperature up to 550°C. Though the films are crystallized, PZT is not oriented and piezoelectric coefficient  $e_{31,f}$  is significantly lower than that of typical PZT on platinized Si substrate [13]. On the contrary, Hua et al. recently reported very encouraging results about sol-gel PZT films deposited on ITO/glass substrate. While the PZT film is

not oriented and the resistance sheet of the 500 nm thick ITO bottom electrode is increased by a factor 10 after annealing at 650°C, the PZT stack shows transparency of around 75 % and excellent piezoelectric performances [8]. However, an optimization of the process is required for controlling the PZT film orientation, and maybe also for decreasing the ITO bottom electrode thickness.

An alternative way for getting optimal PZT on transparent electrode is to use film transfer processing [15]. In that case, the optimal PZT stack grown on suitable substrate is transferred to a host substrate following various possible techniques (grinding of the donor substrate [16], etching of sacrificial layer between PZT and the grown substrate [17-20], laser lift-off [21]). More details about transfer processing can be found in the review paper of Song et al. [22].

In this paper, we report the fabrication and characterization of fully transparent PZT based membranes. An innovative layer transfer process is introduced. It allows obtaining PZT thin film with state of the art properties on top of ITO coated SiO<sub>2</sub> membrane. To the best of our knowledge, this is the first demonstration of functional transparent PZT piezoelectric membranes.

## 2. Experimental

The process used in this work consists in transferring the PZT film from a growth 200 mm Si substrate to a host 200 mm substrate (also Si here), together with additional layers like transparent electrode film (ITO). It is described hereafter and illustrated in Fig. 1. Firstly, state-of-the-art thin film PZT is deposited on a donor platinized Si wafer following standard deposition process already available in MEMS industry. In our case, 1.16 μm thick PZT with Zr/Ti ratio of 52/48 is coated by chemical solution deposition (CSD) using a commercial PZT sol-gel solution provided by Mitsubishi Materials Corporation. Details about the deposition process can be found elsewhere [23]. Then, 150 nm thick ITO electrode layer is sputter deposited on top of the PZT film, followed by 500 nm of SiO<sub>2</sub> as bonding layer (BL). The layer stack on the donor substrate is thus as followed: SiO<sub>2</sub> (BL)/ITO/PZT/Pt/SiO<sub>2</sub>/Si bulk (Fig. 1a). The only major difference with standard PZT stack is the absence of adhesion layer between Pt (100 nm) and SiO<sub>2</sub> (500 nm). Indeed, since Pt does not bond well to SiO<sub>2</sub>, a thin adhesion layer, made usually of TiO<sub>2</sub> or ZrO<sub>2</sub>, is mandatory. The low energy interface (~ 1 J/m<sup>2</sup>) between Pt and SiO<sub>2</sub> will eventually allow easily detaching the PZT stack from the donor wafer by mechanical separation. The receiver Si substrate is made of an 8.5 μm thick SiO<sub>2</sub> film that will play the role of mechanical membrane. Before bonding both wafers, a chemical-mechanical polishing step, removing around 150 nm of SiO<sub>2</sub> on both wafers, followed by a cleaning step consisting of brush scrubbing with NH<sub>4</sub>OH is done so that to get suitable SiO<sub>2</sub> layer surfaces for subsequent molecular bonding, which is realized immediately after. Once wafers are bonded together, an annealing step is performed at 300°C under O<sub>2</sub> for 2h to strengthen the bonding (Fig. 1b). A surface energy in the range of 2.5-3 J/m<sup>2</sup> is then obtained, which is significantly higher than that of the Pt/SiO<sub>2</sub> interface where the debonding occurs. The quality of the bonding is checked by surface acoustic microscopy (Fig. S1). Then, by inserting a blade between bonded wafers, a sharp separation occurs between Pt and SiO<sub>2</sub> layers (Fig. 1c). A thin blade is first aligned in between both bonded wafers, followed by a larger one (cone shape) to separate the wafers (Fig. S2). The PZT stack is thus transferred onto the host wafer, and the donor wafer can be recycled (Fig. 1d). Finally, the Pt layer is removed by dry etching and an ITO layer, 100 nm thick, is sputter deposited on top of PZT film (Fig. 1e). Piezoelectric membranes are then obtained by patterning top ITO electrodes and etching cavities in the Si bulk by deep reactive ion etching (DRIE).

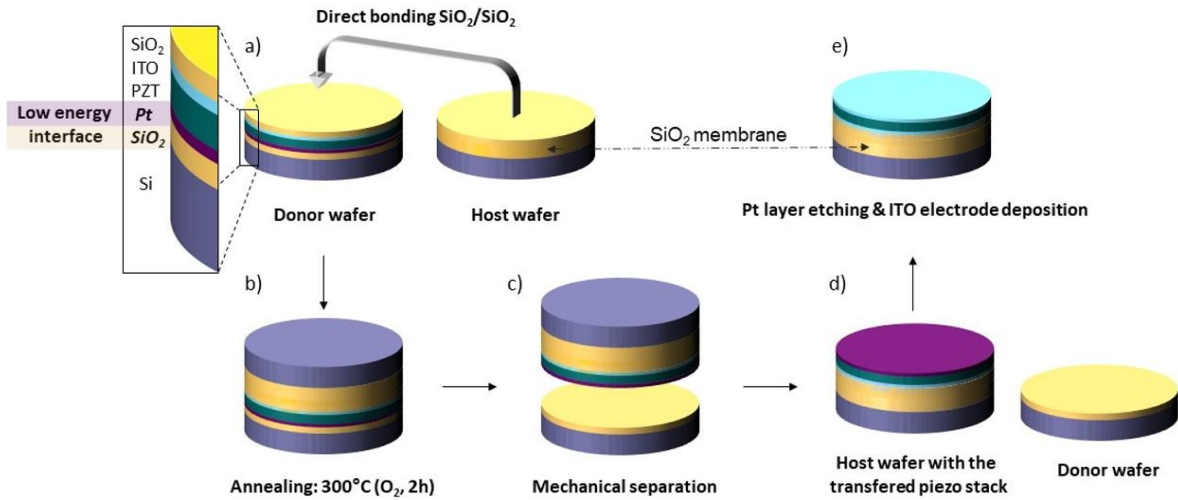
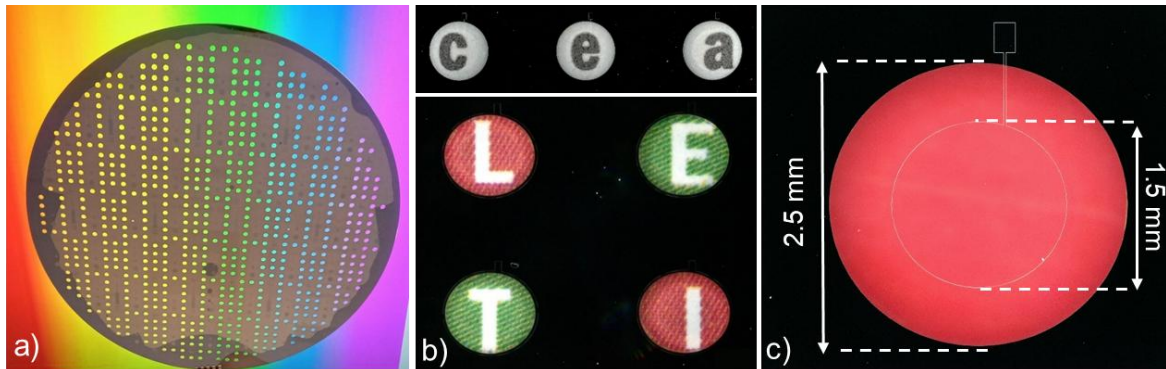


**Fig. 1.** Wafer-to-wafer PZT layer transfer process

The optical transmittance was measured using an Agilent Technologies Spectrophotometer (Cary\_7000). The crystalline structure of the ITO/PZT/ITO stack was characterized by XRD. A scanning electron microscope (SEM) from HITACHI (S-5000) was employed to observe the cross-sectional microstructure of the PZT based membrane. Ferroelectric and dielectric measurements were performed with a TF Analyzer 2000 Measurement System, while displacement measurement was measured with a Double Beam Laser Interferometer (DBLI), both from aixACCT. A Digital Holographic Microscope (DHM), R-2100 from Lyncée Tec was used to measure the out-of-plane displacement of the membrane under applied actuation voltage [24]. Sound Pressure Level (SPL) was obtained using a GRAS 46BE Microphone.

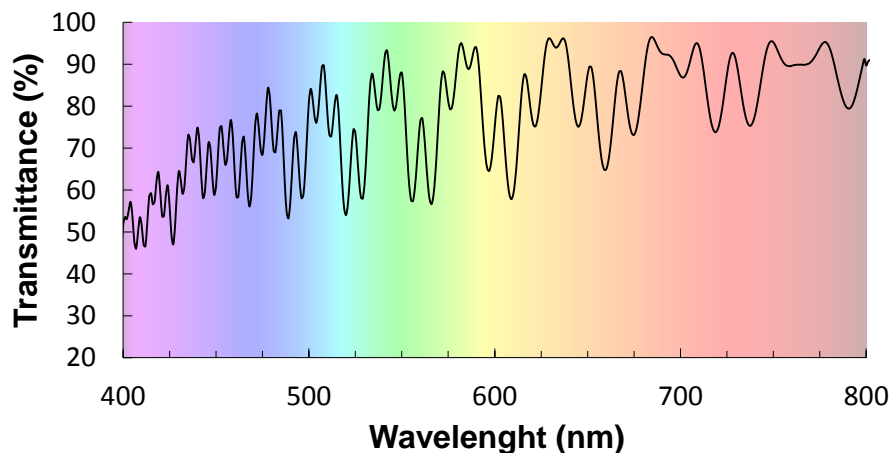
### 3. Results and discussion

Fig. 2a shows a 200 mm silicon wafer with the fabricated PZT based membranes. The PZT stack was transferred on the whole surface except at some punctual bonding defects visible on SAM image (Fig. S1) and at edge of wafer (see Fig. 2a), leading to a yield of PZT transfer > 90 %. The transparency of the ITO/PZT/ITO/SiO<sub>2</sub> stack is evidenced by the clear observation through the membranes of the color spectrum behind the wafer. Another qualitative demonstration of the transparency of the membranes was done using a high-resolution 4K numerical Keyence microscope VHX-7000 (Fig. 2b). Letters printed on a paper are easily readable through the membranes. A close view of the membrane used for all following characterisations is shown Fig. 2c. The diameter of the circular top electrode is 1.5 mm and the cavity made in the bulk silicon, defining the membrane, has a diameter of 2.5 mm.



**Fig. 2.** a) Photograph of a 200 mm Si wafer with transparent PZT based membranes, b) Printed letters through transparent membranes, c) Dimension of the fabricated membrane (top electrode diameter: 1.5 mm; Cavity diameter: 2.5 mm)

The optical transmittance was measured through the centre of various membranes in the visible spectrum (400 nm - 800 nm). The average transmittance is around 75%, as can be seen in Fig. 3. Irregular oscillations are observed on the curve. They are explained by the presence of several interfaces in the PZT capacitor stack where reflections can occur, creating interferences between the different transmitted beams. These quantitative measurements solidify the qualitative proof of transparency evidenced in Fig. 2. An optimisation of the transmission intensity could be performed by tuning the thicknesses of layers or by using anti-reflective layers. Indeed, transmission drops are mainly due to interference issues.



**Fig. 3.** Transmittance spectrum of ITO/PZT/ITO/SiO<sub>2</sub> membrane in the 400-800 nm range.

XRD analysis was performed on the receiving wafer after patterning ITO top electrodes. The theta-2 theta diffractogram shows that PZT exhibits a pure perovskite phase with (100) texturation, as it was after its growth on the donor substrate (Fig. 4). Peaks from ITO are also visible on the XRD pattern. Thus, the thin film transfer process allows obtaining PZT with desired (100) orientation on ITO electrode layer. Indeed, PZT at morphotropic phase boundary with (100) orientation is known to show the highest transverse piezoelectric coefficient  $d_{31}$  [1,25].

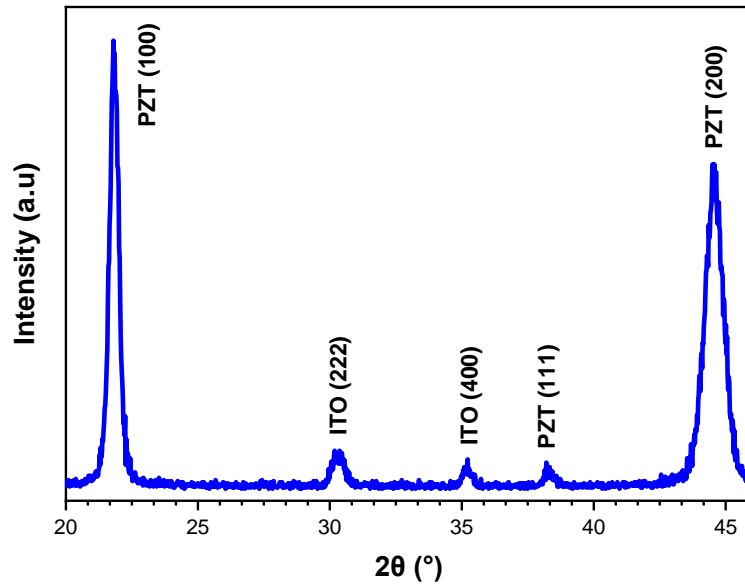


**Fig. 4.** X-ray diffraction pattern of the ITO/PZT/ITO stack (after patterning top ITO).

Fig. 5a is a SEM cross section image of the transferred PZT stack on the host Si wafer. The bonding  $\text{SiO}_2$  bi-layers appears so homogenous that it is not possible to localize the bonding interface, which is a proof of the quality of the bonding. Fig. 5b shows a SEM cross section image with closer view of the ITO/PZT/ITO stack. The PZT film appears dense without apparent voids and cracks. The horizontal lines visible inside the PZT layer result from the RTA crystallization steps that are done every three-coated layers. PZT/ITO interfaces are smooth and clean. The bottom ITO electrode shows a more columnar structure than the upper ITO layer. This might be due to the annealing temperature of  $300^\circ\text{C}$  used for the bonding of wafers in the thin film transfer process. The top ITO film was only annealed at  $190^\circ\text{C}$  after its deposition at room temperature. Note that ITO layers properties were not yet optimized in terms of transparency and electrical conductivity.

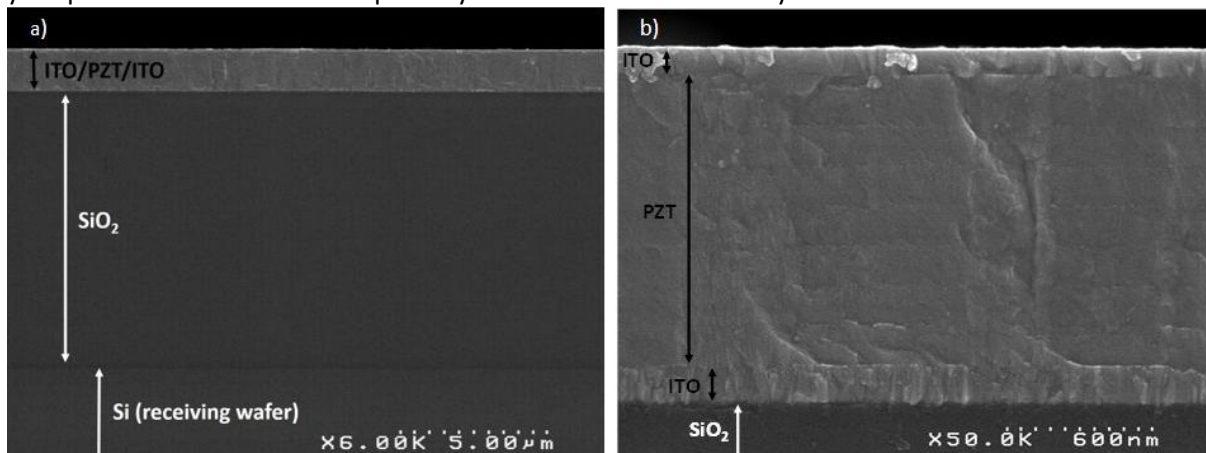


**Fig. 5.** Cross-sectional SEM images of the PZT stack transferred on host Si wafer (a) with closer view of the ITO/PZT/ITO stack (b)

The ferroelectric and dielectric properties measured on a piezoelectric membrane with a PZT capacitor area of 1.81 mm<sup>2</sup> are reported in Fig. 6a and b. The P-E loop measured at 100 Hz shows typical hysteresis shape characteristic of a ferroelectric material. The maximum polarization reaches 40 μC/cm<sup>2</sup> for an applied voltage of 40 V, while the remnant polarization 2P<sub>r</sub> and coercive field 2E<sub>c</sub> are 27 μC/cm<sup>2</sup> and 105 kV/cm, respectively. Capacitance and dielectric losses were registered by sweeping DC voltage between -25 V and +25 V while applying an AC excitation signal (1 kHz, 150 mV). They both show the expected butterfly curve. The maximum permittivity is around 1140 and the dielectric losses are below 15 %. The transverse piezoelectric coefficient d<sub>31</sub> was then calculated using the equation 1 [26]:

$$d_{31}(E) = 2 \cdot \epsilon_r(E) \cdot P(E) \cdot Q \quad (1)$$

Where Q is the electrostriction coefficient (0.04 C<sup>2</sup>/m<sup>4</sup>) [27]. Starting from the polarization and permittivity values previously measured on the membrane, we plot the d<sub>31</sub>-E hysteresis curve shown on Fig. 6c. A maximum d<sub>31</sub> value of about 128 pm/V was calculated, in agreement with typical values reported in literature for PZT 52/48. Fig. 6d shows the large-signal displacement response of the PZT film measured on a clamped 1.81 mm<sup>2</sup> capacitor. The ITO top electrode was coated with 20 nm thick Au film, while backside Si substrate was polished, so that to get reflective surfaces, as required for DBLI measurement. An effective piezoelectric coefficient d<sub>33,f</sub> of 110 pm/V was calculated at 30 V. All those electrical properties are comparable to standard PZT film of equivalent thickness with metal electrodes.

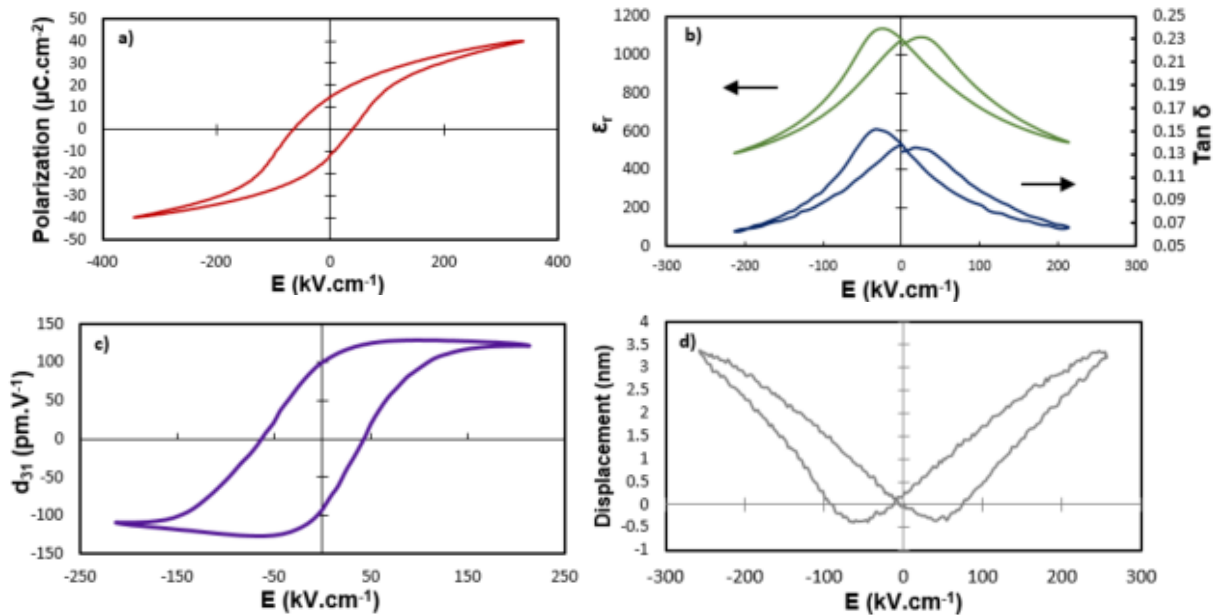


**Fig. 6.** a) Polarization, b) Dielectric permittivity  $\epsilon_r$  and losses  $\tan \delta$ , c) Piezoelectric coefficient  $d_{31}$  and d) Displacement as a function of electric field.

The static deflection of the actuator membranes under applied electric field was measured using Digital Holographic Microscopy. The DHM saves amplitude and phase information of light, which enables recording the displacement of the membrane at different bias. Amplitude gives contrast to create a 2D image, whereas phase gives information about the altitude of any point of the obtained image. This allows plotting a curve of relative displacement of the centre of the membrane as a function of the applied electric field, as reported in Fig. 7. A downward displacement, as expected for disk shape actuator, was observed with a maximum displacement of around 15 μm under an applied voltage of 36 V. Moreover, the displacement curve shows a hysteresis shape, as expected for ferroelectric PZT based actuators.

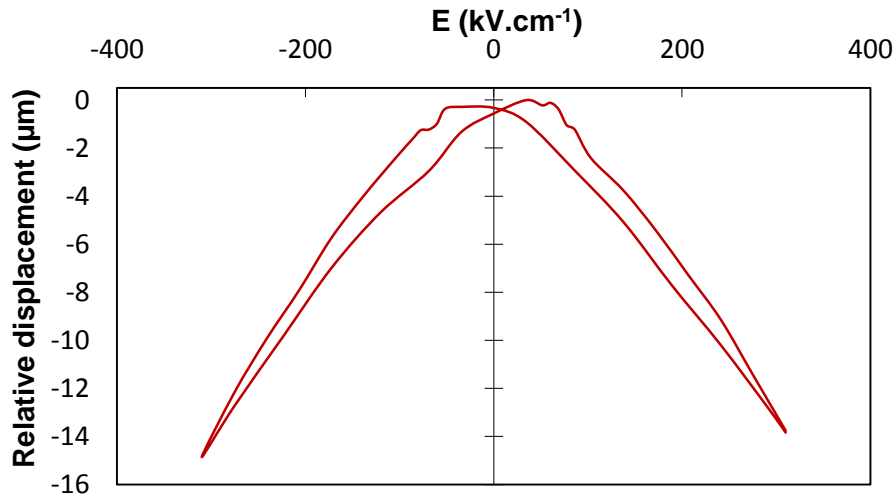


Fig. 7. Relative vertical displacement of the centre of the membrane under applied electric field

As micro-membrane can be used as an ultrasound transducer, we recorded the sound pressure level (SPL) generated by our transparent piezoelectric membrane under suitable electrical excitation signal. The SPL was obtained using a GRAS 46BE Microphone at 1 cm of the measured membrane, using a 15 V input exponential sine sweep with a 15 V<sub>DC</sub> offset and a sampling frequency of 192 kHz. We obtained reproducible results after measuring membranes at 5 different locations on the wafer (Fig. 8). Peaks between 2 and 4 kHz could be linked to the non-anechoic conditions of the setup, while peaks around 50 kHz and 80 kHz mode are due to resonances of the membranes. An acceptable sound pressure level around 80 dB<sub>SPL</sub> is measured. It opens the way for future transparent PMUT devices, for example for gesture recognition or proximity detection.

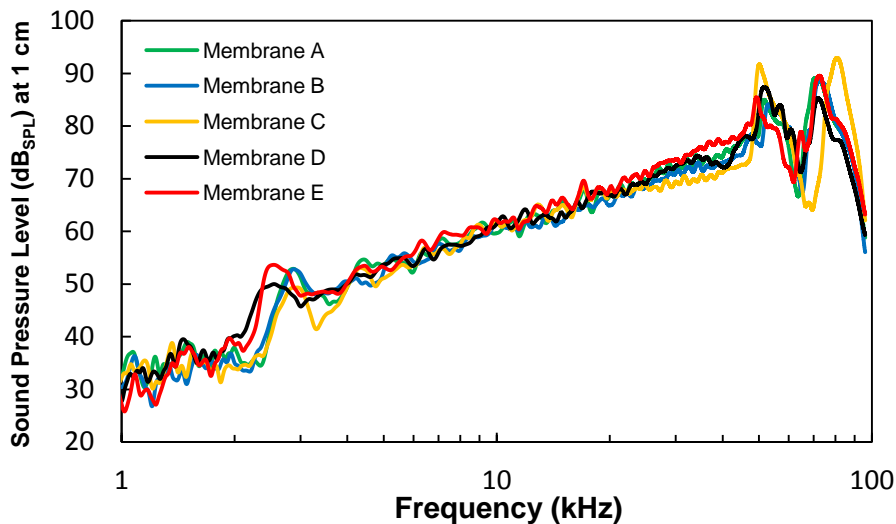


Fig. 8. SPL measured at 1 cm between 1 kHz and 100 kHz on five membranes (1/12 octave smoothing).

#### 4. Conclusion

In conclusion, we have successfully demonstrated the fabrication of transparent PZT based membranes. A 1.16 μm-thick PZT film was integrated between bottom and top ITO electrodes thanks to an innovative film transfer process. The piezoelectric membranes show an average transparency of around 75 % in the visible light range. The ITO/PZT/ITO capacitors show ferroelectric, dielectric and piezoelectric properties similar to PZT MIM structures made of metal electrodes. In particular a

high  $d_{33,f}$  piezoelectric coefficient of 110 pm/V was measured. Piezoelectric actuation of the fabricated membranes was observed using both static deflection and acoustic measurements. These results open the way to the fabrication of transparent Piezoelectric Micromachined Ultrasonic Transducers (PMUT) devices, for example for fingerprint or gesture recognition applications.

## Acknowledgments

The authors thank Catherine Brunet-Manquat and Hugo Dansas for their assistance in taking images at Keyence and SEM, respectively.

## References

- [1] P. Muralt, « Recent Progress in Materials Issues for Piezoelectric MEMS », *J. Am. Ceram. Soc.*, vol. 91, n° 5 (2008) 1385- 1396, doi: 10.1111/j.1551-2916.2008.02421.x.
- [2] C. B. Eom, S. Trolier-McKinstry, « Thin-film piezoelectric MEMS », *MRS Bull.*, vol. 37, n° 11 (2012) 1007- 1017, doi: 10.1557/mrs.2012.273.
- [3] Yole Développement, Piezoelectric Devices: From Bulk to Thin-Film (Yole Développement, 2019), [https://www.slideshare.net/Yole\\_Developpement/piezoelectric-devices-from-bulk-to-thinfilm-2019-report-by-yole-dveloppement](https://www.slideshare.net/Yole_Developpement/piezoelectric-devices-from-bulk-to-thinfilm-2019-report-by-yole-dveloppement)
- [4] H. Chen, S. Mirg, M. Osman, S. Agrawal, J. Cai, R. Biskowitz, J. Minotto, S. Kothapalli, « A High Sensitivity Transparent Ultrasound Transducer Based on PMN-PT for Ultrasound and Photoacoustic Imaging », *IEEE Sens. Lett.*, vol. 5, n° 11 (2021) 1- 4,doi:10.1109/LSENS.2021.3122097.
- [5] G. Thalhammer, C. McDougall, M. P. MacDonald, M. Ritsch-Marte, « Acoustic force mapping in a hybrid acoustic-optical micromanipulation device supporting high resolution optical imaging », *Lab. Chip*, vol. 16, n° 8 (2016) 1523- 1532, doi: 10.1039/C6LC00182C.
- [6] R. Manwar, K. Kratkiewicz, K. Avnani, « Overview of Ultrasound Detection Technologies for Photoacoustic Imaging », *Micromachines*, vol. 11 (2020) Art. n° 7, doi: 10.3390/mi11070692.
- [7] S. Glinsek, M. Aymen Mahjoub, M. Ruppin, T. Schenck, N. Godard, S. Girod, J. Chemin, R. Leturcq, N. Valle, S. Klein, C. Chappaz, E. Defay « Fully Transparent Friction-Modulation Haptic Device Based on Piezoelectric Thin Film », *Adv. Funct. Mater.*, vol. 30 (2020) 2003539, doi: 10.1002/adfm.202003539.
- [8] H. Hua, Y. Chen, Y. Tao, D. Qi, Y. Li, « A highly transparent haptic device with an extremely low driving voltage based on piezoelectric PZT films on glass », *Sens. Actuators A*, vol. 335 (2022) 113396, doi: 10.1016/j.sna.2022.113396.
- [9] M. Shehzad, S. Wang, Y. Wang, « Flexible and transparent piezoelectric loudspeaker », *Npj Flex. Electron.*, vol. 5 (2021) 24, doi: 10.1038/s41528-021-00121-z.
- [10] I. Boerasu, L. Pintilie, M. Pereira, M. I. Vasilevskiy, M. J. M. Gomes, « Competition between ferroelectric and semiconductor properties in Pb(Zr<sub>0.65</sub>Ti<sub>0.35</sub>)O<sub>3</sub> thin films deposited by sol-gel », *J. Appl. Phys.*, vol. 93, n° 8 (2003) 4776- 4783, doi: 10.1063/1.1562009.
- [11] V. Zardetto, T. M. Brown, A. Reale, A. D. Carlo, « Substrates for flexible electronics: A practical investigation on the electrical, film flexibility, optical, temperature, and solvent resistance properties », *J. Polym. Sci. Part B Polym. Phys.*, vol. 49 (2011) p. 638- 648, doi: 10.1002/polb.22227.
- [12] H. Kim, C.M. Gilmore, A. Piqué, J.S. Horwitz, H. Mattoussi, H. Murata, Z.H. Kafafi, D.B. Chrisey, « Electrical, optical, and structural properties of indium-tin-oxide thin films for organic light-emitting devices », *J. Appl. Phys.*, vol. 86 (1999) 6451- 6461, doi: 10.1063/1.371708.
- [13] K. Ueda, S.-H. Kweon, H. Hida, Y. Mukouyama, I. Kanno, « Transparent piezoelectric thin-film devices: Pb(Zr, Ti)O<sub>3</sub> thin films on glass substrates », *Sens. Actuators Phys.*, vol. 327 (2021) 112786, doi: 10.1016/j.sna.2021.112786.

- [14] T. D. Cheng, N. J. Zhou, P. Li, « Ferroelectric and photoelectricity properties of (Pb<sub>0.52</sub>Zr<sub>0.48</sub>)TiO<sub>3</sub> thin films fabricated on FTO glass substrate », *J. Mater. Sci. Mater. Electron.*, vol. 26, (2015) 7104- 7108, doi: 10.1007/s10854-015-3332-5.
- [15] G. Le Rhun, C. Dieppedale, B. Wagué, C. Querne, G. Enyedi, P. Perreau, P. Montméat, C. Licitra, S. Fanget, « Transparent PZT MIM Capacitors on Glass for Piezoelectric Transducer Applications », in *2019 20th International Conference on Solid-State Sensors, Actuators and Microsystems Eurosensors XXXIII (TRANSDUCERS EUROSENSORS XXXIII)* 1800- 1802. doi: 10.1109/TRANSDUCERS.2019.8808241
- [16] R. Guerre, U. Dreschler, D. Bhattacharyya, P. Rantakari, R. Stutz, R. V. Wright, Z. Milosavljevic, T. Vaha-Heikkila, P. B. Kirby, M. Despont, « Wafer-Level Transfer Technologies for PZT-Based RF MEMS Switches », *J. Microelectromechanical Syst.*, vol. 19, n° 3, p. 548- 560, doi: 10.1109/JMEMS.2010.2047005.
- [17] T. Liu, M. Wallace, S. Troler-McKinstry, T. N. Jackson, « High-temperature crystallized thin-film PZT on thin polyimide substrates », *J. Appl. Phys.*, vol. 122, n° 16, p. 164103, doi: 10.1063/1.4990052.
- [18] T. Samoto, H. Hirano, T. Somekawa, K. Hikichi, M. Fujita, M. Esashi, S. Tanaka , « Wafer-to-wafer transfer process of barium strontium titanate for frequency tuning applications using laser pre-irradiation », *J. Micromechanics Microengineering*, vol. 25, n° 3, p. 035015, doi: 10.1088/0960-1317/25/3/035015.
- [19] Y. Qi, N. T. Jafferis, K. Lyons, C. M. Lee, H. Ahmad, M. C. McAlpine, « Piezoelectric Ribbons Printed onto Rubber for Flexible Energy Conversion », *Nano Lett.*, vol. 10, n° 2, p. 524- 528, doi: 10.1021/nl903377u.
- [20] K.-I. Park, S. Y. Lee, S. Kim, J. Chang, S.-J. L. Kang, K. J. Lee, « Bendable and Transparent Barium Titanate Capacitors on Plastic Substrates for High Performance Flexible Ferroelectric Devices », *Electrochem. Solid-State Lett.*, vol. 13, n° 7, p. G57, doi: 10.1149/1.3407622.
- [21] M. Kousuke, M. Moriyama, M. Esashi, S. Tanaka, « Low-voltage PZT-actuated MEMS switch monolithically integrated with CMOS circuit », in *2012 IEEE 25th International Conference on Micro Electro Mechanical Systems (MEMS)*, p. 1153- 1156. doi:10.1109/MEMSYS.2012.6170367.
- [22] L. Song, S. Glinsek, E. Defay, « Toward low-temperature processing of lead zirconate titanate thin films: Advances, strategies, and applications », *Appl. Phys. Rev.*, vol. 8 (2021) 041315, doi: 10.1063/5.0054004.
- [23] S. Fanget, F. Casset, S. Nicolas, C. Dieppedale, M. Allain, B. Desloges, G. Le Rhun, « Piezoelectric actuators, next driver for MEMS market? », *TechConnect Briefs*, vol. 4 (2017) 64- 67.
- [24] Y. Emery, T. Colomb, E. Cuhe, « Metrology applications using off-axis digital holography microscopy », *J. Phys Photonics*, vol. 3 (2021) doi: 10.1088/2515-7647/ac0957.
- [25] M. Cueff, M. Allain, J. Abergel, G. Le Rhun, M. Aid, E. Defay, D. Faralli, « Influence of the crystallographic orientation of Pb(Zr,Ti)O<sub>3</sub> films on the transverse piezoelectric coefficient d<sub>31</sub> », in *2011 IEEE International Ultrasonics Symposium* 1948- 1951. doi:10.1109/ULTSYM.2011.0485.
- [26] M. Nakajima, S. Okamoto, H. Nakaki, T. Yamada, "Enhancement of piezoelectric response in (100)/(001) oriented tetragonal Pb(Zr,Ti)O<sub>3</sub> films by controlling tetragonality and volume fraction of the (001) orientation", *J. Appl. Phys.* 109, 091601 (2011)
- [27] M. Cueff, PhD Thesis from University of Grenoble (2011)